

## The Added Value of Diffusion Weighted MR Images in Assessment of Benign Prostatic Lesions and Prostatic Carcinoma

Shimaa H.I Desouky, Amir Hanna, \*Asmaa Monir Aly, Rehab Mohamed Shimy, Mona H Hassan

Radiology Department, Theodor Bilharz Research Institute

\*Corresponding author: Asmaa Monir Aly, Email: asmaa\_monir@hotmail.com

### ABSTRACT

**Background:** Prostate cancer is considered the most common malignant neoplasm in males worldwide and the 2<sup>nd</sup> important reason for cancer-related male deaths after bronchogenic carcinoma.

**Objective:** The purpose of this research is to assess how diffusion weighted image (DWI) and apparent diffusion coefficient (ADC) value characterise prostatic cysts, senile prostatic hyperplasia, prostate cancer, and the normal prostatic gland.

**Patients and methods:** We enrolled 60 cases with suspicious prostatic lesions, 20 cases with benign prostatic hypertrophy, 20 cases prostate cancer and 20 with prostatic cyst along with 20 controls. All underwent magnetic resonance imaging (MRI) for prostatic assessment and Trans-rectal ultrasonography (TRUS) guided biopsy.

**Results:** Prostate cancer had a considerably lower mean ADC value ( $p$ -value  $< 0.001$ ) than normal central gland (CG), peripheral zone (PZ), and benign prostatic hyperplasia (BPH) nodules. The ADC value of the PZ tissue had been substantially higher than that of the normal central zone (CZ) ( $p < 0.001$ ). While the prostatic cyst's ADC value was much greater than CZ's ( $p < 0.001$ ), the BPH lesion's ADC value had been significantly lower than CZ's ( $p < 0.001$ ).

**Conclusions:** DWI has been a useful tool for gathering information on the tissue properties of the prostate's various anatomical zones. In contrast to normal tissue, BPH, and prostate cysts, prostate carcinoma cause restricted diffusion of water, which may be used in the differential diagnosis of benign and malignant lesions.

**Keywords:** Diffusion-weighted Images, ADC value, Prostatic cancer, Prostatic cyst, Benign prostatic hyperplasia.

### INTRODUCTION

After bronchogenic carcinoma, prostate cancer is thought to be the most frequent malignant tumor in men worldwide and the 2<sup>nd</sup> leading reason for cancer-related mortality in men. It is still vitally necessary to employ noninvasive imaging investigations that can increase tumor specificity and retain excellent sensitivity<sup>(1)</sup>.

Digital rectal examination had anatomical limitations decreasing the sensitivity of the examination<sup>(2)</sup>. Transrectal ultrasound has the advantage of direct visualization of the prostatic pathologies, yet it has some limitations such as its operator dependence, lack of specificity, poor characterization and lesional localization. Multidetector computed tomography examinations can evaluate the size of swollen glands and the creation of abscess cavities, but they are unable to distinguish between benign and malignant diseases<sup>(3)</sup>.

MR imaging techniques have the advantages of multiplanar imaging and high soft tissue contrast resolution and can be used in patients with senile prostatic lesions such as prostatic cysts and prostatic adenoma and can help differentiation from prostate cancer<sup>(4)</sup>.

Prostate cancer shows low T2-weighted images (WI) signal intensity compared to the normal high signal intensity of the normal peripheral zone. It also displays low T1 WI signal, which has not been specific

for cancer as it is also seen in benign conditions, like chronic prostatitis, hyperplastic prostatic nodules, prostatic atrophy, scarring, post-radiotherapy, post-therapeutic sequelae and in post-biopsy hemorrhagic changes that all may simulate tumoral tissue<sup>(5)</sup>.

Certain prostatic tumors involving the central gland have been difficult to distinguish from benign nodules of low signal intensity associated with prostatic hyperplasia on T2 weighted imaging, making it difficult to detect them<sup>(6)</sup>.

Functional MR imaging methods, such as diffusion-weighted imaging, are the most useful and user-friendly<sup>(7)</sup>. In addition to being easier to process after imaging, they don't require the administration of intravenous (IV) contrast and can be acquired faster than proton MR spectroscopy, requiring less training from technologists to execute<sup>(8)</sup>. Its disadvantages include being susceptible to motion and magnetic field inhomogeneities artifacts<sup>(7)</sup>.

When compared to non-cancerous tissue, prostate cancer tissue typically exhibits more restricted diffusion<sup>(9)</sup>. Lesions with prostate cancer are observed to have lower ADC values than prostatic parenchyma that is normal<sup>(10)</sup>.

As a result, DWI and ADC are effective markers for assessing prostatic tissue and distinguishing among benign prostatic tissue, ageing prostatic lesions, and prostatic cancer<sup>(11)</sup>.

Our study aimed to assess the DWI appearance and ADC value in characterization of the normal

## **PATIENTS and METHODS**

### ***Patients:***

From January 2021 to July 2023, 60 specimens, from all studied cases who visited the Radiology Department with a history of prostatic problems, were included in the research. We enrolled 60 studied cases with suspicious prostatic lesions and were categorized as 20 cases with benign prostatic hypertrophy, 20 cases with prostate cancer and 20 studied cases with prostatic cyst along with 20 healthy controls.

All patients underwent magnetic resonance imaging (MRI) study for prostatic assessment either before or after Trans-rectal ultrasonography (TRUS) guided biopsy. The difference in time among biopsy and MRI was one month instead of twenty days. No patient had ever received heat therapy, hormone therapy for the prostate, chemotherapy, or pelvic irradiation.

**Inclusion criteria:** We included patients with suspected pathology on digital rectal examination or any detected central or peripheral nodule on ultrasound examination and complaints of lower urinary tract symptoms, like dysuria, frequent micturition, urgency, weak stream, and retention of urine or gross hematuria as well as estimated/elevated prostatic specific antigen (PSA) level.

**Exclusion criteria:** We exclude any patients who had a general contraindication to MRI like those patients with pacemakers, cochlear implants, and other electromagnetic implants in the body as well as claustrophobia and non-available histopathological data.

### ***Histopathological Analysis***

The histopathology was reviewed by an experienced pathologist.

### ***MRI imaging:***

MR imaging had been performed using 1.5-Tesla or more MRI machines (Philips Achieva 1.5 and 3 Tesla, made in USA), with a pelvic phased array coil to cover the whole prostate.

The following parameters were used to acquire a conventional T2 weighted fast spin-echo to the prostate in the axial, sagittal, and coronal planes, as well as in the three orthogonal planes: FOV 16 cm<sup>2</sup>, acquisition matrix 152 x 114, number of continuous slices 30, interslice gap 0.5 mm, slice thickness 3 mm, FSE 5870/90 ms [TR/effective TE], echo train length sixteen, number of signal averages 1.5; total acquisition time 12 minutes.

Utilizing the following parameters, axial T1-

prostatic gland, prostate carcinoma, prostatic cysts and senile prostatic hyperplasia. weighted turbo spin-echo pictures were produced: Acquisition time: four minutes; TSE 400/10 ms [TR/effective TE], NSA 6. FOV 16 cm<sup>2</sup>, acquisition matrix 256x150; number of continuous slices: 20; interslice gap: 0.5 mm; slice thickness: 3 mm.

### ***Diffusion study:***

Echo-planar diffusion-weighted sequences (DWI 3862/73 [TR/TE]) with b values of 1000, 1200, and 1400 s/mm<sup>2</sup> were performed transversely to the prostate. The phase-encoding gradient had been from left to right. The number of contiguous slices was 30, slice thickness 4 mm, FOV 20 cm<sup>2</sup>, acquisition matrix 80 x 65 with an image acquisition time of 2 minutes 24 seconds.

### ***ACD mapping:***

Regions of interest (ROIs) were created for the chosen regions on the ADC maps. The ADC maps were recreated after the DWI datasets were moved to a separate workstation for post-processing. ROI was created to calculate the ADC value of the periphery and central zones of the prostate gland. ROIs were placed in the PZ and CZ, respectively. After drawing ROIs into the primary prostatic cancer (Pca) foci and BPH nodules in the BPH and prostate cancer lesions, ADCs were computed.

To reduce any errors in the ADC calculation, care had been taken to exclude the urethra and neurovascular bundle when drawing the ROI.

### ***MRI image analysis:***

These criteria were used to identify prostate cancer in MR images:

- Low signal intensity in T2-weighted images explained high DWI signal intensity than the rest of the prostate and low signal intensity in ADC map images, which is also used to identify the lesions not well identified by T2 and DWI.
- A central gland nodule with variable high or low signal strength was identified as BPH.
- Evaluations for prostate cancer included looking for involvement of the seminal vesicles, invasion of the neurovascular bundles, breaching of the prostatic capsule, the existence of metastatic pelvic lymph nodes, and bone deposits of the pelvic bones.
- The sites of the lesions were identified as either peripheral, central, or transitional and also as either mid, basal, or apical.
- For prostatic cancer, TMN was identified as well as the PIRADS classification.

**Ethical consent:** An approval of the study was obtained from Theodor Bilharz Research Institute (TBRI) Ethical Committee. Every patient signed an informed written consent for acceptance of participation in the study. This work has been carried out in accordance with The Code of Ethics of the World Medical Association (Declaration of Helsinki) for studies involving humans.

### **Statistical analysis**

Statistical analysis had been conducted using SPSS 27<sup>th</sup> edition, categorical variables had been presented in count and percentage and compared among groups using Fisher's exact test. Quantitative variables had been presented in mean, standard deviation, median, minimum and maximum and were compared among groups using Kruskal Wallis test. (Dunn's test is the post-hoc test used) .Receiver operator characteristics (ROC) curve analysis was conducted to assess predictability of ADC value for prostatic lesions compared to healthy controls along with cutoff for diagnosis, sensitivity, specificity and accuracy. Any p value <0.05 had been considered significant.

### **RESULTS**

We enrolled 60 studied cases with suspicious prostatic lesions and were categorized as twenty studied cases with benign prostatic hypertrophy, 20 studied cases with prostate cancer and twenty studied cases with prostatic cyst along with 20 healthy controls. Table 1 shows the comparison of demographics and radiological

characteristics between study groups.

Comparison of age showed that prostate cancer and BPH group were significantly older compared to prostatic cyst, and healthy controls. Pairwise comparison presented that main differences were between control versus prostatic cancer and controls versus BPH.

PSA levels were significantly different between groups, pairwise comparison explained that main differences were between control versus prostatic cancer and controls versus BPH.

There had been statistically significant difference among groups in terms of distribution of lesions within gland, prostatic cancers were mainly found in the peripheral zones unilateral or bilateral, while BPH was mainly found in the central zone affecting right side more than left, prostatic cysts were exclusively in the central zone.

Diffusion weighted MRI showed that BPH lesions majorly showed no restriction of diffusion (80%), all prostatic cancer cases showed high signal (70%), and prostatic cysts showed mainly no restrictions in 80% of cases.

ADC values were significantly different between groups, with the highest levels reported in prostatic cysts, followed by controls, then BPH, and the lowest in prostate cancer. Pairwise comparison showed that control vs prostatic cyst, control vs BPH, control vs prostate cancer, prostatic cyst vs prostate cancer, and BPH vs prostate cancer presented statistically significant differences.

**Table (1): Comparison of demographics and radiological characteristics between study groups.**

		Group								
		BPH		Prostate cancer		Prostatic cyst		Control		
		Mean ±SD	Median (Min-Max)	Mean ±SD	Median (Min-Max)	Mean ±SD	Median (Min-Max)	Mean ±SD	Median (Min-Max)	P value
<b>Age</b>	Years	66.8±8.8	69 (46-77)	66.5±10.1	71 (46-77)	54.9±14.9	56 (31-72)	45±15.6	42.5 (26-71)	<0.001
<b>PSA</b>	ng/dL	11±3.3	11.8 (6-14.5)	12.4±3.1	14 (6-15.8)	7.8±5.1	8.4 (0-15.8)	6±2.4	5 (4-11.5)	<0.001
		Count	%	Count	%	Count	%	Count	%	
<b>Site of lesion</b>	No lesion	0	0%	0	0%	0	0%	20	100%	<0.001
	Bilateral peripheral zone	2	10%	4	20%	0	0%	0	0%	
	Infiltrative lesion infiltrating all gland	0	0%	1	5%	0	0%	0	0%	
	Left central zone	6	30%	1	5%	10	50%	0	0%	
	Left peripheral zone	0	0%	6	30%	0	0%	0	0%	
	Right central zone	8	40%	0	0%	10	50%	0	0%	
	Right peripheral zone	4	20%	8	40%	0	0%	0	0%	
<b>Diffusion</b>	High signal	0	0%	14	70%	0	0%	0	0%	<0.001
	Mild high	0	0%	2	10%	0	0%	0	0%	
	Mild restriction	2	10%	0	0%	0	0%	0	0%	
	Moderate high signal	0	0%	4	20%	0	0%	0	0%	
	No diffusion	2	10%	0	0%	4	20%	20	100%	
	No restriction	16	80%	0	0%	16	80%	0	0%	
<b>ADC value</b>	10 <sup>3</sup>	1.31±0.15	1.31 (1.11-1.59)	0.9±0.2	0.9 (0.4-1.1)	2.9±0.4	2.9 (2.5-3.6)	1.7±0.2	1.8 (1.4-1.9)	<0.001
<b>Correlate with pathology</b>	Proven	0	0.00%	14	70.00%	0	0.00%	0	0.00%	<0.001
	Proven cyst	0	0.00%	0	0.00%	20	100.00%	0	0.00%	
	Proven hyperplasia	18	90.00%	0	0.00%	0	0.00%	0	0.00%	
	Proven BPH only by pathology	2	10.00%	0	0.00%	0	0.00%	0	0.00%	
	Proven pathology	0	0.00%	4	20.00%	0	0.00%	0	0.00%	
	Proven with capsular tissue	0	0.00%	2	10.00%	0	0.00%	0	0.00%	
<b>Diagnosis by pathology</b>	Negative	0	0%	0	0%	0	0%	20	100%	<0.001
	Positive	20	100%	20	100%	20	100%	0	0%	
<b>Diagnosis by MRI</b>	Negative	2	10%	0	0%	0	0%	20	100%	<0.001
	Positive	18	90%	20	100%	20	100%	0	0%	

Pairwise Comparisons of Group	Age	PSA	ADC
	P value	P value	P value
Control-prostatic cyst	0.323	0.248	0.029
Control-BPH	<0.001	0.001	<0.001
Control-prostate cancer	<0.001	<0.001	<0.001
Prostatic cyst-BPH	0.100	0.369	0.068
Prostatic cyst-Prostate cancer	0.069	0.012	<0.001
BPH-prostate cancer	1	1	0.029

SD: Standard deviation ADC: Apparent diffusion coefficient, BPH: benign prostatic hyperplasia, PSA: prostatic specific antigen, PZ: peripheral zone, SD: standard deviation, MRI: Magnetic resonance imaging.

Table 2 shows that, regarding prostate cancer patients, Gleason score was 7 in 17 (85%) patients, group 2 was found in 10 (50%) patients. PIRADS V was reported in 10 (50%) patients, and as for primary tumor staging, T2b was found in 40%.

**Table (2 ): Characteristics of prostate cancer patients.**

		Count	%
<b>Gleason score</b>	7	17	85.0%
	8	3	15.0%
<b>Group</b>	Group 2	10	50.0%
	Group 3	7	35.0%
	Group 4	3	15.0%
<b>PIRADS</b>	III	2	10.0%
	IV	8	40.0%
	V	10	50.0%
<b>Stage</b>	T2a	2	10.0%
	T2b	8	40.0%
	T2c	2	10.0%
	T3b	6	30.0%
	T3C	2	10.0%

PIRADS: Prostate Imaging Reporting and Data System.

ADC values could significantly predict BPH compared to controls with AUC 97%, p value <0.001, cutoff value  $\leq 1.44$ , with sensitivity of 90% and of specificity 90% (Figure 1).

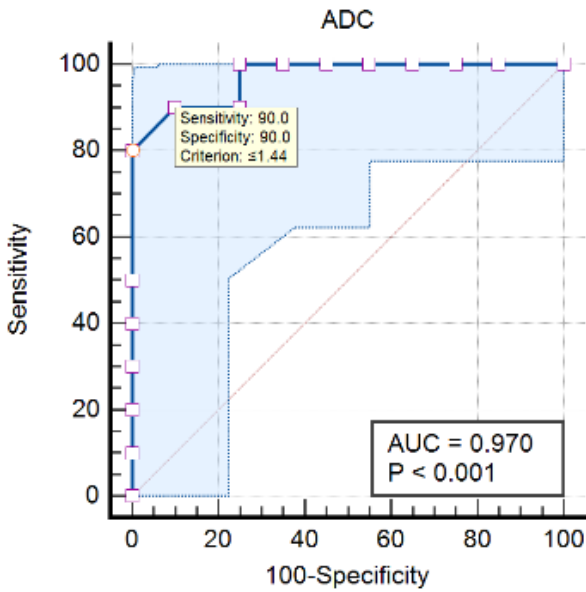


**Figure (1):** ROC curve showed predictability of ADC values for benign prostatic hyperplasia

ADC values could significantly predict prostate cancer compared to controls with AUC 100%, p value <0.001, cutoff value  $\leq 1.05$ , with sensitivity of 100% and specificity of 100% (Figure 2).

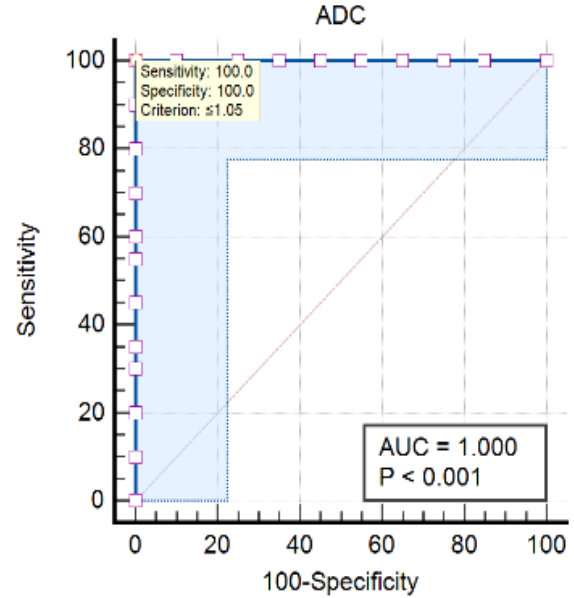


**Figure (2):** ROC curve showed predictability of ADC values for prostate cancer.

ADC values could significantly predict prostatic cyst compared to controls with AUC 100%, p value <0.001, cutoff value  $\leq 1.927$ , with sensitivity of 100% and specificity of 98% (Figure 3).

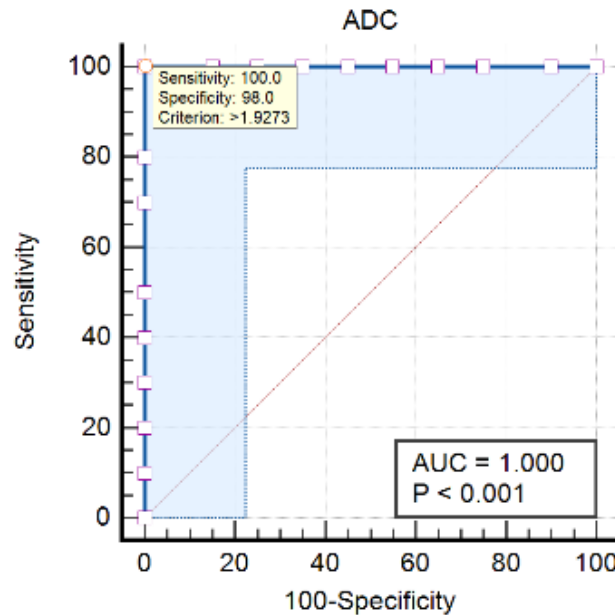


**Figure (3):** ROC curve showed predictability of ADC values for BPH.

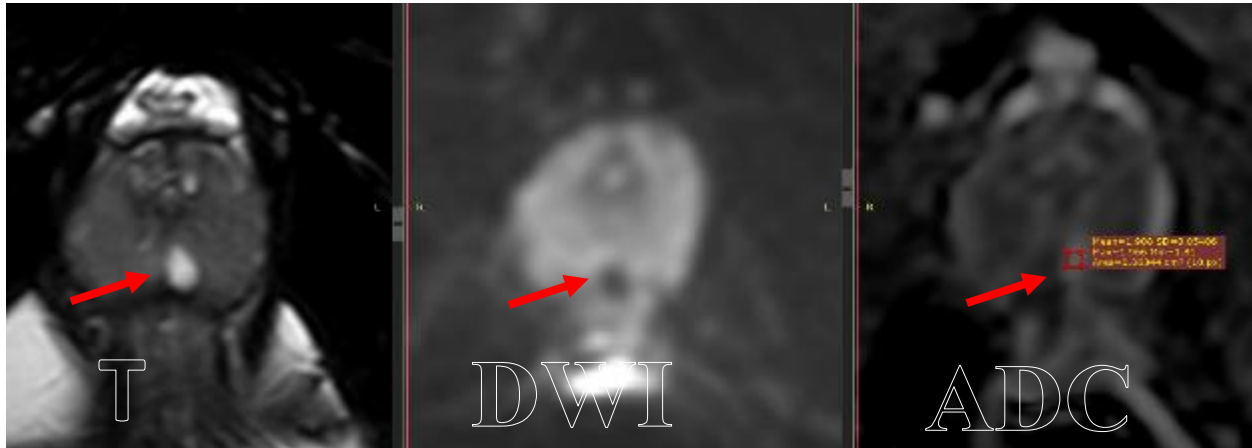


**Figure (4):** 23-years-old male patient with symptoms of prostatitis. Posterior prostatic cyst left paramedian line in location at the level of the mid gland displaying high T2 signal with low DWI signal and high ADC value (red arrows). The mean ADC value is  $1.9 \pm 0.054$ .



**Figure (5):** BPH in a 66-year-old male, PSA level 3.2 ng/mL (a) Axial T2 WI of the prostate showing enlarged heterogeneous CG and right central zone base of the gland hypertrophied parenchymal nodule (b) no diffusion restriction (c) mild low signal in ADC map, the calculated ADC value is  $1.243 \times 10^{-3} \text{ mm}^2/\text{s}$ .

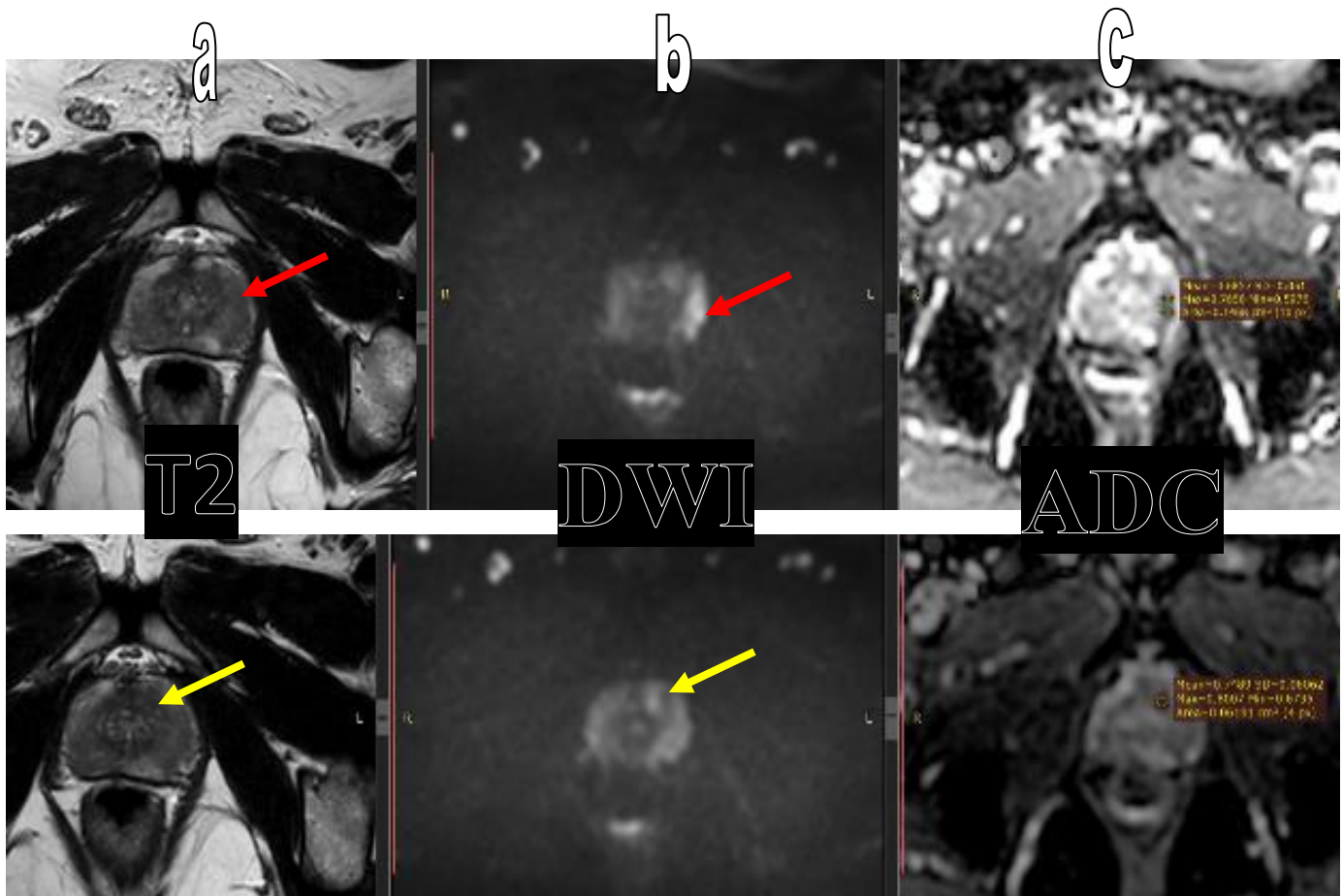


**Figure (6):** PCa in a 64-year-old male, PSA level 38.6 ng/mL, Gleason score 2+ 3. (a) Axial T2 WI of the prostate showing small hypointense lesion in the left side of the PZ (**red arrow**) and left transitional zone (**yellow arrow**). (b) Diffusion WI and (c) ADC map show restricted diffusion of the lesions, with the ADC value being  $0.6857 \times 10^3$  and  $0.7489 \times 10^3 \text{ mm}^2/\text{s}$ .

## DISCUSSION

This research study enrolled 60 patients who had history of prostatic problems aiming to clarify the role of MRI in differentiating different prostatic lesions.

We found that ADC values for the normal PZ, CG, BPH, and PCa in this investigation were comparable to those described in the literature. The mean ADC values were  $1.843 \times 0.168 \times 10^{-3} \text{ mm}^2/\text{sec}$  and  $1.636 \times 0.243 \times 10^{-3} \text{ mm}^2/\text{sec}$  for normal PZ and CG respectively. This was consistent with research by **Emad-Eldin et al.**<sup>(12)</sup> and **Tamada et al.**<sup>(13)</sup>, which found that the normal CG was  $1.469 \times 0.2391 \times 10^{-3} \text{ mm}^2/\text{sec}$ , and the normal PZ had a mean ADC value of  $1.839 \times 0.233 \times 10^{-3} \text{ mm}^2/\text{sec}$ . According to **Ren et al.**<sup>(14)</sup>, mean ADC values of normal PZ and CG were  $1.829 \times 10^{-3} \text{ mm}^2/\text{sec}$  and  $1.352 \times 10^{-3} \text{ mm}^2/\text{sec}$ ,

respectively. According to **Liu et al.**<sup>(15)</sup>, the normal PZ and CG had ADC values of  $1.69 \pm 0.28 \times 10^{-3} \text{ mm}^2/\text{sec}$  and  $1.36 \pm 0.12 \times 10^{-3} \text{ mm}^2/\text{sec}$ , respectively.

In the current research prostatic cysts showed the highest ADC value  $2.9 \pm 0.4 \times 10^{-3}$ . Solid lesions displayed restricted diffusion, while these lesions demonstrated enhanced diffusion. This was consistent with the earlier outcome by **Ren et al.**<sup>(14)</sup> who claimed that cysts exhibit more signal attenuation on higher b value diffusion images, while cellular tissues, like tumors, exhibit restricted diffusion (high signal intensity) on these images.

Benign prostatic hyperplasia had a mean ADC value of  $1.31 \pm 0.15 \times 10^{-3} \text{ mm}^2/\text{sec}$ . This outcome had been consistent with that of **Emad-Eldin et al.**<sup>(12)</sup> who found a mean ADC value of  $1.359 \pm 0.201 \times 10^{-3} \text{ mm}^2/\text{sec}$  for 20 studied cases with BPH. Nevertheless,



this had been a little lower than the value previously published by **Ren et al.**<sup>(14)</sup> for twenty-nine patients with BPH had been  $1.576 \pm 0.099 \times 10^{-3} \text{ mm}^2/\text{sec}$ .

Compared to normal CG, the ADC value of BPH had been substantially lower. This was consistent with the earlier results of **Emad-Eldin et al.**<sup>(12)</sup> and **Liu et al.**<sup>(15)</sup>. **Manaia et al.**<sup>(16)</sup> found that this may be because CG tissue from BPH studied cases has a higher stroma tissue content and a lower glandular component content than healthy CG tissue.

The average ADC value for prostatic carcinoma was discovered to be  $0.9 \pm 0.2 \times 10^{-3} \text{ mm}^2/\text{sec}$ . This was consistent with earlier findings of **Emad-Eldin et al.**<sup>(12)</sup> They stated that the average ADC value for twenty prostatic cancer studied cases had been  $0.87 \pm 0.13 \times 10^{-3} \text{ mm}^2/\text{sec}$  and **Ren et al.**<sup>(14)</sup> found that the average ADC value for twenty-one prostatic cancer studied cases had been  $0.934 \pm 0.166 \times 10^{-3} \text{ mm}^2/\text{sec}$ . An additional investigation conducted by **Tanimoto et al.**<sup>(17)</sup> said that the average PCa ADC value had been  $0.93 \pm 0.11 \times 10^{-3} \text{ mm}^2/\text{sec}$ . But it had been marginally less than the amount that had been previously disclosed by **Kiliçkesmez et al.**<sup>(18)</sup> They discovered that the nine Pca studied cases' mean ADC value had been  $1.06 \pm 0.17 \times 10^{-3} \text{ mm}^2/\text{sec}$ . Additionally, it had been less than the worth of **Tamada et al.**<sup>(13)</sup> who recorded  $1.02 \pm 0.25 \times 10^{-3} \text{ mm}^2/\text{sec}$  as the mean ADC value. However, it was marginally greater than the figure that had been previously disclosed by **Abdel Maboud et al.**<sup>(19)</sup>. They discovered that 31 PCa cases had a mean ADC value of  $0.737 \pm 0.154 \times 10^{-3} \text{ mm}^2/\text{sec}$ .

With a  $p$  value  $>0.0001$ , the ADC values of benign and malignant prostatic lesions differed significantly, supporting earlier results reported by **Yağcı et al.**<sup>(20)</sup> who have proved that there is a significant statistical difference among benign and malignant tissue with  $p$  value  $< 0.001$ . **Tamada et al.**<sup>(13)</sup> further demonstrated that benign lesions had higher mean ADC values than malignant lesions, and that these differences were statistically significant with  $p$  values of less than 0.001. Research carried out by **Kiliçkesmez et al.**<sup>(18)</sup> stated that the ADC values of the normal peripheral zone, central zone, and prostatic carcinomas were statistically significantly different with a  $p$  value  $< 0.05$ . **Ren et al.**<sup>(14)</sup> have reported that with  $p$  values  $< 0.05$ , the mean and standard deviation ADC values for the PZ, PCA foci, BPH nodules, and normal central zone were statistically significantly different.

Our study has limitations as the pelvic phased array coils used led to lower signal to noise ratio(SNR) in the prostate region and, thus, lower image quality.

Additionally, the blood flow through the microscopic blood vessels adds to the determination of the ADC value. Increased ADC value brought on by increased vascular flow to the lesion in the event of a dominant intra-prostatic lesion may offset the anticipated decline in ADC value brought on by increasing cellularity. Combining DW-MRI images with high enough b-values to guarantee that perfusion impacts are eliminated can help separate the ADC related to extracellular fluid from that resulting from perfusion.

## CONCLUSION

The outcomes of our investigation demonstrated that DWI has been a useful tool for gathering information on the tissue properties of the prostate's various anatomical zones. In contrast to normal tissue, BPH, and prostate cysts, prostate carcinoma may cause restricted diffusion of water. This can lead to increased signal intensity on DWI and reduced ADC values, which may be used in the differential diagnosis of benign and malignant lesions. This will be a promising approach in clinical practice.

- **Funding:** No funding.
- **Conflict of interest:** Nil.

## REFERENCES

1. **Kim I (2019):** Commentary on local therapy in men who present with a metastatic prostate cancer from special issue senior guest editor. American Journal of Clinical and Experimental Urology, 7(2): 61–63.
2. **Naji L, Randhawa H, Sohani Z et al. (2018):** Digital rectal examination for prostate cancer screening in primary care: A systematic review and meta-analysis. The Annals of Family Medicine, 16(2):149-154.
3. **Giganti F, Rosenkrantz A, Villeirs G et al. (2019):** The evolution of MRI of the prostate: The past, the present, and the future. American Journal of Roentgenology, 213(2):384-396.
4. **Eze B, Mbaeri T, Oranusi KC et al. (2019):** Correlation between intravesical prostatic protrusion and international prostate symptom score among Nigerian men with benign prostatic hyperplasia. Nigerian Journal of Clinical Practice, 22(4):454-459.
5. **Panda A, Gulani V (2020):** MRI appearance of prostate cancers in locations posing diagnostic or biopsy challenges. In: Reading MRI of the Prostate. Springer, Pp: 59-66.
6. **Fütterer J(2017):** Multiparametric MRI in the detection of clinically significant prostate cancer. Korean Journal of Radiology, 18(4):597-606.
7. **Korn N (2019):** A multiparametric MRI for the classification and grading of prostate. Cancer Diss UCSF., 7(1) :2-3.
8. **Alexander E, Murray J, Morgan V et al. (2019):**

- Validation of T2- and diffusion-weighted magnetic resonance imaging for mapping intra-prostatic tumor prior to focal boost dose-escalation using intensity-modulated radiotherapy (IMRT). *Radiotherapy and Oncology*, 141:181-187.
9. **Tamada T, Kido A, Takeuchi M *et al.* (2019):** Comparison of PI-RADS version 2 and PI-RADS version 2.1 for the detection of transition zone prostate cancer. *European Journal of Radiology*, 121:108704.
  10. **Kapur S, Das C, Sharma S (2019):** Multiparametric magnetic resonance imaging of the prostate: An update. *Annals of the National Academy of Medical Sciences (India)*, 55:74–83
  11. **Bajgiran A, Mirak S, Sung K *et al.* (2019):** Apparent diffusion coefficient (ADC) ratio versus conventional ADC for detecting clinically significant prostate cancer with 3-T MRI. *American Journal of Roentgenology*, 213(3):134-142.
  12. **Emad-Eldin S, Halim M, Metwally L *et al.* (2014):** Diffusion-weighted MR imaging and ADC measurement in normal prostate, benign prostatic hyperplasia and prostate carcinoma. *The Egyptian Journal of Radiology and Nuclear Medicine*, 45(2):535-542.
  13. **Tamada T, Sone T, Toshimitsu S *et al.* (2008):** Age-related and zonal anatomical changes of apparent diffusion coefficient values in normal human prostatic tissues. *Journal of Magnetic Resonance Imaging*, 27(3):552-6.
  14. **Ren J, Huan Y, Wang H *et al.* (2008):** Diffusion-weighted imaging in normal prostate and differential diagnosis of prostate diseases. *Abdominal Imaging*, 33(6):724-8.
  15. **Liu X, Peng W, Zhou L *et al.* (2013):** Biexponential apparent diffusion coefficients values in the prostate: comparison among normal tissue, prostate cancer, benign prostatic hyperplasia and prostatitis. *Korean Journal of Radiology*, 14(2):222-232.
  16. **Manaia J, Cardoso G, Pires L *et al.* (2020):** Three-dimensional organization of the pars fibroreticularis framework of the urethral wall in normal human prostates. *Archives of Medical Science*, 16(5):1057-1061.
  17. **Tanimoto A, Nakashima J, Kohno H *et al.* (2007):** Prostate cancer screening: the clinical value of diffusion-weighted imaging and dynamic MR imaging in combination with T2-weighted imaging. *Journal of Magnetic Resonance Imaging*, 25(1):146-52.
  18. **Kiliçkesmez O, Cimilli T, Inci E *et al.* (2009):** Diffusion-weighted MRI of urinary bladder and prostate cancers. *Diagnostic Interventional Radiology*, 15(2):104-10.
  19. **Abdel Maboud N, Elsaid H, Aboubeih E (2014):** The role of diffusion-weighted MRI in evaluation of prostate cancer. *The Egyptian Journal of Radiology and Nuclear Medicine*, 45(1):231–236.
  20. **Yağcı A, Ozari N, Aybek Z *et al.* (2011):** The value of diffusion-weighted MRI for prostate cancer detection and localization. *Diagnostic Interventional Radiology*, 17(2):130-134.